

Membership Inference Attacks for Unseen Classes

Pratiksha Thaker Neil Kale Zhiwei Steven Wu Virginia Smith
Carnegie Mellon University
{pthaker, nkale, zstevenwu, smithv}@cmu.edu

Abstract

Shadow model attacks are the state-of-the-art approach for membership inference attacks on machine learning models. However, these attacks typically assume an adversary has access to a background (nonmember) data distribution that matches the distribution the target model was trained on. We initiate a study of membership inference attacks where the adversary or auditor cannot access an entire subclass from the distribution—a more extreme but realistic version of distribution shift than has been studied previously. In this setting, we first show that the performance of shadow model attacks degrades catastrophically, and then demonstrate the promise of another approach, quantile regression, that does not have the same limitations. We show that quantile regression attacks consistently outperform shadow model attacks in the class dropout setting—for example, quantile regression attacks achieve up to $11\times$ the TPR of shadow models on the unseen class on CIFAR-100, and achieve nontrivial TPR on ImageNet even with 90% of training classes removed. We also provide a theoretical model that illustrates the potential and limitations of this approach.

1 Introduction

Membership inference attacks (MIAs) are powerful tools to assess the privacy of models trained on potentially sensitive data [11, 2]. MIAs take advantage of the fact that models tend to memorize training data, so that even when a model generalizes relatively well, its loss on training examples is likely to be systematically lower than the loss on similar examples *not* in the training data. Given a target model f trained on data assumed to be sampled i.i.d. from a distribution P , a typical MIA operates by training proxy models using a similar architecture and training procedure on “background” data sampled from P but known to be disjoint from the training data of f .

In practice, an auditor or adversary is unlikely to have sample access to a distribution that is identical to P and disjoint from the training data of f , and may instead only have samples from some shifted distribution P' . This distribution shift can take many forms [11, 2, 19, 9, 5]. In this paper, we focus on a case that has not been studied in prior work—where an auditor would like to test whether the training data may contain examples from some class i , but *cannot sample from class i* when training the attack model(s) using samples from P' .

This is not a contrived setting. Our work is motivated by the important yet challenging problem of detecting sensitive content such as child sexual abuse material (CSAM) in a model’s training data [14, 15, 7, 16]. Here, MIAs could be useful to flag potentially offending models for further scrutiny [16]. However, due to legal and ethical restrictions, auditors are often unable to directly access examples of CSAM to train proxy models for membership inference [14]. Such restrictions are also reasonable to assume for other real-world applications of AI safety, where the sensitive content being queried may either be inaccessible or unpreferred for use during training. However, even in less restricted scenarios, it is not uncommon for imbalance to exist between classes in the proxy training data due simply to data scarcity constraints—mimicking the class drop out setting for rare classes.

The state-of-the-art approach for MIAs is to train a large number of *shadow models* [2] (models that aim to mimic the behavior of the target model but are trained on controlled subsets of data) in order to model the target model’s behavior when a given sample is or is not in the training data. This attack trains several models on nonmember data to solve the same task as the target model, and then uses these as proxies to decide whether the point is more likely to be a member or nonmember in the target.

In this work, we show that shadow models may fail catastrophically when performing membership inference in the unseen class setting. Shadow models crucially rely on training models that *perform the same task as the target model*, and with no samples from class i , a classifier may assign zero probability to label i , causing the classification task to fail on samples from the unseen class.

To solve this problem, we instead explore an approach based on *quantile regression*, which has been used recently for computationally efficient membership inference attacks [1, 13]. The key observation is that unlike shadow models, which learn the target score distribution indirectly by training several models that must perform well on the target task, quantile regression directly learns the score distribution of the target model, bypassing the learning problem solved by the target model (e.g., classification). Overall, we make the following contributions:

- We formalize the problem of performing membership inference attacks with classes not seen at attack time. Our work is motivated by data scarcity constraints as well as practical AI safety scenarios such as the detection of child sexual abuse material (CSAM), where legal or ethical concerns limit the ability of auditors to use data from sensitive classes to train proxy models [14].
- When performing MIA with unseen classes, we show that the default approach of training shadow models deteriorates in performance, and instead explore the use of quantile regression as a promising alternative. Our results show that in the 1% FPR regime, quantile regression can achieve up to $11\times$ the TPR of shadow models on the unseen class (on CIFAR-100). Meanwhile, on ImageNet, we find that quantile regression can achieve 3.8% TPR at 1% FPR (about half the TPR achieved by full training) with access to only *10% of training classes*.
- Finally, we provide a theoretical model illustrating the benefits and potential limitations of quantile regression in this setting. Our analysis helps to better explain the effectiveness of the approach and also points to several directions of future study.

2 Background and Preliminaries

In this section, we formalize the membership inference attack (MIA) setting and introduce relevant attack methods.

We begin with the supervised learning setup. Let $\mathcal{D} \in \Delta(\mathcal{X} \times \mathcal{Y})$ denote the data distribution over input features \mathcal{X} and labels \mathcal{Y} . The target model f is trained on a dataset $D_{\text{priv}} \sim \mathcal{D}$ consisting of n_{priv} labeled examples (x_i, y_i) . In the classification setting, we assume \mathcal{Y} is a finite label set with $|\mathcal{Y}| = c$. The model f outputs a vector of logits, i.e., $f: \mathcal{X} \rightarrow \mathbb{R}^c$.

In a membership inference attack, the adversary aims to determine whether a given *target* example (x, y) was part of the private training dataset D_{priv} . The adversary is typically assumed to have access to an auxiliary dataset $D_{\text{pub}} \sim \mathcal{D}$, which is disjoint from the private dataset, i.e., $D_{\text{pub}} \cap D_{\text{priv}} = \emptyset$. However, in this work we consider a practical setting where D_{pub} is drawn from a more restricted sub-population.

Setting: MIA with limited access to classes. In practice, the adversary may only have access to samples from a *subset* of the classes used to train the target model. This can happen for a number of reasons. For example, the background data may be drawn from a public source such as data available on the Internet, while the target model may include samples from private or proprietary data sources. For auditors who want to run MIA to audit a model for potentially harmful content (as in the CSAM example described above [14]), that content may not be legally available to the auditor at large enough scale to train the attack. Alternatively, the adversary may simply be resource-limited and unable to collect representative samples covering the space of data used to train the target model.

Let $Y_d \subseteq \mathcal{Y}$ denote the set of *unseen* classes. In this setting, the adversary has access to a public dataset D'_{pub} drawn from the conditional distribution $\mathcal{D}_{-Y_d} := \mathcal{D} | y \notin Y_d$, which contains only *seen* classes. Despite this restriction, we aim to evaluate the performance of the membership inference attack (MIA) on target examples drawn from the full distribution \mathcal{D} . This setup allows us to study whether MIA methods trained on a restricted subset of classes can generalize to previously unseen classes from the original distribution.

We now introduce three classes of MIA methods. Each method relies on a *score function* s that assigns a numeric score to a target example (x, y) , intended to reflect the likelihood that (x, y) was included in the training set for the model f . For example, in [1, 2], an example of such a score function is based on logit differences:

$$s(x, y, f) = f(x)_y - \max_{y' \neq y} f(x)_{y'} \quad (1)$$

In prior work, this score relies on knowledge of the true label. In this work, we also evaluate a score function based on the difference of the top two logits (agnostic to the label) and report results in the subsequent sections.

1) Marginal baseline attack with a single threshold. The marginal baseline attack [18] is a simple yet widely used baseline for membership inference. Here, the attacker chooses a single threshold τ such that any example (x, y, f) with $s(x, y) > \tau$ is predicted to be a member of D_{priv} , and otherwise it is predicted to be a non-member. In our setting, we compute this threshold based on the held-out public dataset D'_{pub} . Specifically, the threshold τ is chosen to control the false positive rate (FPR) over D'_{pub} . Note that the FPR computed over D'_{pub} may not accurately reflect the FPR under the distribution \mathcal{D} due to the distribution shift.

2) Shadow model attack. Unlike the simple marginal baseline attack, the shadow model attack (and quantile regression attack) considers performing MIA with per-example thresholds. In particular, the shadow model attack [11, 2] constructs a reference distribution over model outputs to evaluate membership of a target example. Formally, the adversary trains k shadow models g_1, \dots, g_k , each solving the same classification task as the target model f , with architecture and training procedure identical to that of f , and trained using the same algorithm as f .

In our setting, each shadow model is trained on random subsets drawn independently from the public dataset D'_{pub} . In keeping with the computationally tractable “offline” attack in Carlini et al. [2], for each target point, we only use the set of shadow models for which the training point is a *nonmember*. (We note that Carlini et al. [2] evaluate both the online and offline attacks and show that the difference in the ROC curves is minimal.) The collection of shadow models allows the attacker to learn the conditional distribution of the scores:

$$P_{\text{out}} : s(x, y, g) \mid (x, y) \text{ is not used in training } g$$

Given the target model f , the attacker decides membership based on the probability of the score $s(x, y, f)$ under P_{out} .

3) Quantile regression attack. The quantile regression attack [1, 13] offers an efficient alternative to shadow model approaches for membership inference. Rather than fitting a distribution over shadow model outputs, the attacker directly learns a function that maps input examples to score thresholds—thereby enabling per-example thresholds. Given a target FPR α , the attacker trains a model $q_\alpha : \mathcal{X} \times \mathcal{Y} \rightarrow \mathbb{R}$ to estimate the $(1 - \alpha)$ -quantile of the score distribution, conditioned on the input (x, y) . The model q_α is trained via minimizing the *pinball loss* over a function class \mathcal{H} on the public dataset

$$q_\alpha \in \arg \min_{q' \in \mathcal{H}} \mathbb{E}_{(x, y) \sim D'_{\text{pub}}} [\text{PB}_{1-\alpha}(q'(x), s(x, y, f))] \quad (2)$$

where $\text{PB}_{1-\alpha}$ is defined as $\text{PB}_{1-\alpha}(\hat{s}, s) = \max\{\alpha(\hat{s} - s), (1 - \alpha)(s - \hat{s})\}$. This loss function is well known to elicit quantiles, in the same way that squared loss elicits means. Then the MIA predicts membership if $s(x, y, f) > q_\alpha(x)$.

When the function class \mathcal{H} consists only of constants, the quantile regression attack reduces to the marginal baseline with a fixed threshold. More generally, a flexible function class allows the attacker to adapt thresholds on a per-example basis. Notably, this approach requires training only a single, lightweight model unlike shadow model attacks, which often demand replicating the full training pipeline and architecture of the target model.

3 Shadow Models Fail on Unseen Classes

We first show that the state-of-the-art approach to membership inference—training shadow models—fails in the class dropout setting.

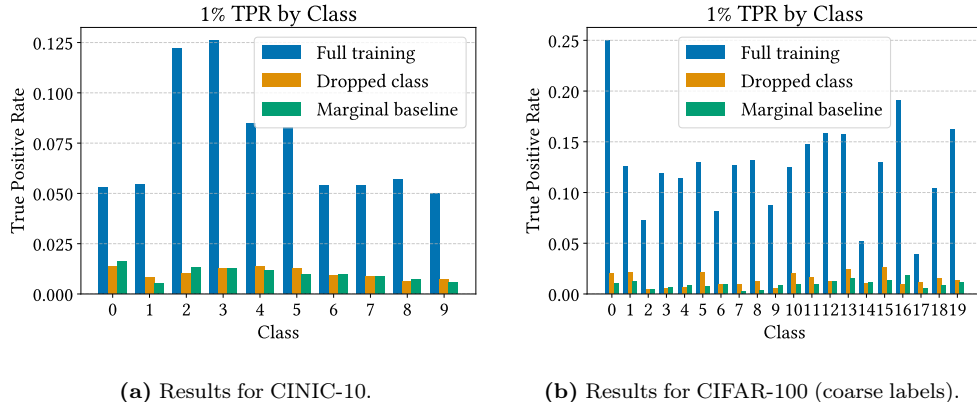


Figure 1: True positive rates for shadow model attacks in the 1% false positive rate regime for CINIC-10 and CIFAR-100 (we defer the 0.1% regime to Appendix B). Each bar represents the TPR on the indicated class. In yellow, we plot the TPR when that class is excluded from shadow model training. The attack success degrades significantly under class exclusion, often performing worse than the marginal baseline (global threshold).

Setup. We assume a setting where the target model is trained on half the training data, the adversary has access to all but one class (from the remaining training data) to train the attack, and the query points are drawn from the unseen class.

For each attack, we train 16 shadow models using the “offline” variant of the LiRA algorithm with a fixed, global variance estimate. (Due to computational constraints, we limit our attack to 16 models, but Carlini et al. [2] note that “With a global estimate of the variance, the attack performs nearly on par with our best attack with as little as 16 shadow models,” making this a reasonable baseline. We do not expect our results to improve with more shadow models.) We use the LiRA attack unmodified except that the shadow models’ training data excludes examples from the unseen class.

We train shadow models on CINIC-10 and CIFAR-100 (using the superclass label set consisting of 20 classes). In Figure 1 we report the performance of shadow models on queries from each class before and after dropping a single class at a time. We find that for both datasets, shadow models perform on par with a much weaker marginal baseline that does not learn per-example thresholds but rather fits a single threshold across all classes.

Intuitively, a model that does not see a class at training time will assign zero probability to that class label. As a result, the shadow models’ confidences for the true label on the missing class will be zero, resulting in many false positives at test time—any higher confidence reported by the target model would be considered significant.

The attack in Carlini et al. [2] as stated relies on being able to estimate the probability of the correct label for the query example for each shadow model. This may not be a fundamental limitation of the approach. For example, one could also use a different score function, such as the difference between the top two logits agnostic to the true label. We find that using this score function does not significantly improve the performance of shadow models in the class-dropout setting (in fact, it reduces the baseline performance of the attack even without dropping classes) – we plot these results in Figure 2. Thus, for the remainder of our comparisons, we use the true label confidence as the score function for shadow models.

4 Quantile Regression Attacks for Unseen Classes

Shadow models are fundamentally constrained because they must solve the same learning problem as the target model in order to estimate the score distribution of the target model on a given example. In contrast, quantile regression attacks aim to directly learn the score (or difficulty) distribution of the target model itself on nonmember data in order to predict per-example score thresholds. In other words, the task of quantile regression is to learn a representation of the data that correlates well with the difficulty of each example (but this does not require solving the same task as the target model). The key takeaway from our results is that in some cases, this representation can be learned adequately from only a subset of examples, even when some classes have zero support.

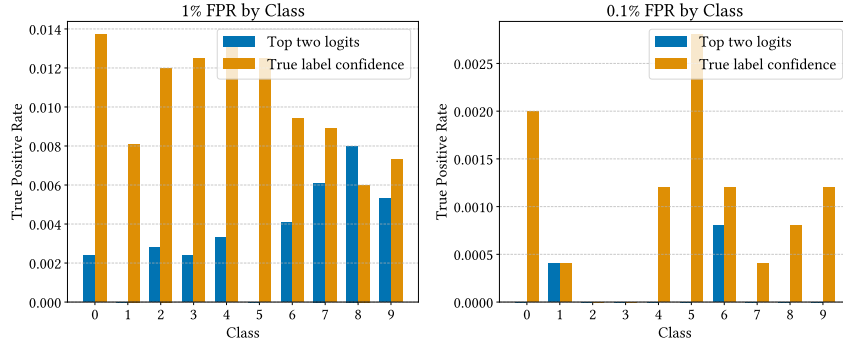


Figure 2: Comparison between shadow model attack success (with class i dropped) with true label confidence as the score metric and top-two logit difference as the score metric on CINIC-10. Although the top-two logit difference does not use the true (dropped) label that was not seen by the shadow models, the attack performs even worse than with the true label confidence.

4.1 Quantile regression attack performance on unseen classes.

We now present our main results showing that quantile regression attacks outperform shadow models and global thresholding on unseen classes.

Setup. We first study an identical setting where the target Resnet50 base model is trained on half the training data, the adversary has access to all but one class from the remaining training data to train the attack, and the query points are drawn from the unseen class.

For each attack, we train a single quantile regression model on the remaining training data, excluding the unseen class and keeping the validation set as heldout public data for evaluating FPR. Pinball loss is notoriously difficult to minimize, so for training stability, we follow Bertran et al. [1] and train the network to fit a Gaussian (mean and variance) conditioned on each sample instead of directly using pinball loss to predict quantiles.

Our final models for the CINIC-10 and CIFAR-100 attacks are ConvNext-Tiny-224 models trained for 30 epochs, with the Adam optimizer, batch size 16, and learning rate of 1e-4. We find that early stopping does not improve the attacks. To make our attack agnostic to the true label, we modify the attack from Bertran et al. [1] and use the difference between the top two logits as our score function:

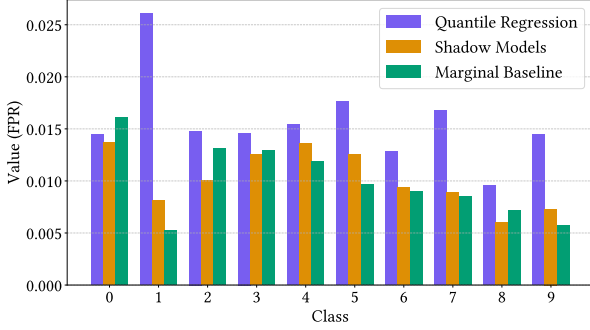
$$s(x,y,g) = \max f(x) - \max_{y' \neq \max f(x)} f(x)_{y'}.$$

Using this score function improves quantile regression performance in the class dropout setting as the learned attack no longer requires knowledge of the true label.

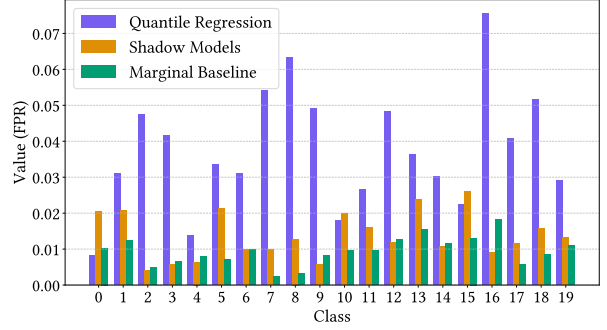
Class dropout: CINIC-10 and CIFAR-100. We find that for both CINIC-10 and CIFAR-100 (using the superclass label set), quantile regression strictly outperforms the marginal baseline and shadow models under class dropout at 1% FPR. In this setting, we train the model on all classes except one, so 9 classes for CINIC-10 and 19 superclasses for CIFAR-100. The TPR and FPR are evaluated on the held-out class. For CINIC-10, the quantile regression attack generalizes better on some unseen classes such as automobiles (1) and trucks (2) than others.

Results are similar on CIFAR-100 but even more pronounced. On average across all 20 superclasses, shadow models achieve only 1.4% TPR at 1% FPR on unseen data while quantile regression achieves 3.8% TPR at 1% FPR. While in-distribution, shadow models (12.5% TPR at 1% FPR) significantly outperform quantile regression (4.1% TPR at 1% FPR), in the class dropout setting, quantile regression takes less time to train and outperforms shadow models.

Data scarcity: ImageNet. Our results on CINIC-10 and CIFAR-100 are limited to a single unseen class at a time, which simulates the impact of a minority subpopulation (such as sensitive or harmful content) missing



(a) TPR for the dropped out class, CINIC-10



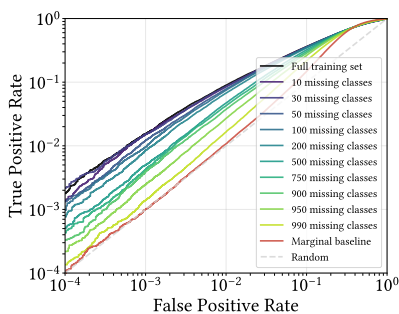
(b) TPR for the dropped out class, CIFAR-100

Figure 3: True positive rates in the low false positive regime for CINIC-10 and CIFAR-100 (superclass set) on each unseen class. Each bar represents the true positive rate on class i when class i is dropped from the attack training set. We only report results at 1% FPR; the results at 0.1% FPR are not meaningful due to the small sample size of the validation set on a single class (1000 samples). While quantile regression attacks have only a small advantage over shadow models on CINIC-10, they achieve up to $11\times$ higher TPR than shadow models on CIFAR-100.

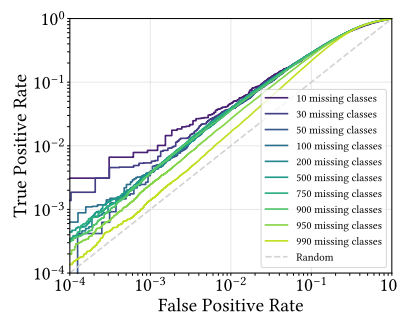
from the attack data. Another realistic scenario where the auditor or adversary might not have access to subclasses is the *data scarcity* setting, where the model might be trained using a much larger and potentially proprietary dataset while a resource-limited auditor only has a fraction of similar data available.

To simulate this, we attack a model trained on the much larger ImageNet dataset. We use the same quantile regression architecture and hyperparameters as described for CINIC-10 and CIFAR-100. In Figure 4a, we show the ROC curves for ImageNet (on the full data distribution) with a sweep from 10 to 990 classes missing from the attack training set. Perhaps surprisingly, the quantile regression attack outperforms the marginal baseline with as many as 990 out of 1000 classes left unseen.

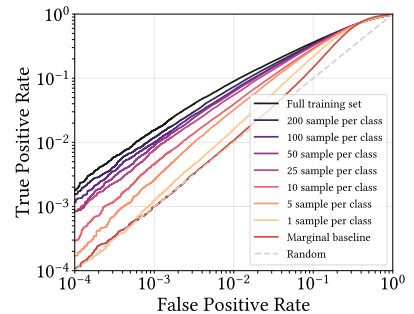
One might ask whether this effect is simply due to averaging over both missing and in-distribution classes. In Figure 4b, we plot attack performance for the missing classes alone. The performance on unseen classes remains fixed around 3.8% TPR at 1% FPR (0.4% TPR at 0.1% FPR) when anywhere from 100 to 900 classes are removed, and remains significantly above the marginal baseline even with 990 classes removed.



(a) ROC curve for class drop experiment on ImageNet.



(b) Unseen class ROC curve for class drop experiment on ImageNet.



(c) ROC curve for sample drop experiment on ImageNet.

Figure 4: ROC curves for class and sample drop experiments on ImageNet.

Finally, another realistic setting of data scarcity is one where examples from all classes are available, but where the auditor only has very few samples from each class. We also evaluate ImageNet in this scarce-sample setting where only k samples are retained from each class. Quantile regression outperforms the marginal baseline (Figure 4c) even when training data is severely limited, retaining 3.9% TPR at 1% FPR given as few as 10 samples per class (compared to 9.0% TPR at 1% when trained on all the data; on average, 401 samples per class).

5 Theoretical Model

Our empirical results are promising, showing that the quantile regression attack can achieve nontrivial accuracy even under extreme data scarcity when training the attack model. However, it is not clear from our empirical results when we might expect quantile regression to succeed. Indeed, on the CINIC-10 dataset, quantile regression has a relatively small advantage over the baseline approaches.

As a step toward understanding our results, we prove a “transferability” theorem for quantile regressors. Intuitively, this theorem states that if the distribution of samples with and without the unseen classes is “similar,” then the FPR guarantee of the quantile regressor trained on only the seen classes should also hold on the full query set.

Definition 5.1 (Pinball loss). For a quantile level $\alpha \in (0,1)$, the *pinball loss* (also known as the check loss) for a prediction \hat{s} and true outcome s is defined as:

$$\ell_\alpha(\hat{s},s) = (\alpha - \mathbf{1}\{s < \hat{s}\})(s - \hat{s}) = \begin{cases} \alpha(s - \hat{s}) & \text{if } s \geq \hat{s}, \\ (1 - \alpha)(\hat{s} - s) & \text{if } s < \hat{s}. \end{cases}$$

Quantile Regression Predictor. We consider a class of linear quantile regression predictors of the form:

$$q_\alpha(x) = \langle \phi(x), w \rangle,$$

where $\phi: \mathcal{X} \rightarrow \mathbb{R}^d$ is a fixed feature mapping, and $w \in \mathcal{W}$ is a weight vector. For any distribution P over $\mathcal{X} \times \mathcal{S}$, we will write P_ϕ to denote its induced distribution over $(\phi(x), s)$.

We will focus on the case where $\mathcal{W} = \mathbb{R}^d$, but should generalize to more constrained set of weights later. We adapt the multi-accuracy definition [10, 6] to our specific setting with a feature mapping.

Definition 5.2 (Multi-Accuracy for Quantile Prediction). A predictor $q_\alpha: \mathcal{X} \rightarrow \mathbb{R}$ is said to be $(\mathcal{W}, \phi, \varepsilon)$ -*multi-accurate* for quantile level α with respect to distribution P if, for every $w \in \mathcal{W}$,

$$|\mathbb{E}_{(x,s) \sim P}[\langle w, \phi(x) \rangle \cdot (\mathbf{1}\{s < q_\alpha(x)\} - \alpha)]| \leq \varepsilon.$$

We now show that multi-accuracy, when instantiated for quantile prediction, provides a sufficient condition for calibration to transfer across distributions. We consider the setting where a quantile predictor is trained on distribution P and deployed on a shifted distribution Q . The theorem below shows that if the feature representation captures the density ratio between P and Q via a linear function, then the learned predictor remains calibrated at the target quantile level under Q . This result can be viewed as a specialized instance of the *universal adaptability* framework of Kim et al. [8], tailored to multi-accurate quantile predictors derived from empirical risk minimization.

Theorem 5.3 (Transferability of Quantile Predictors). *Let P and Q be distributions over (x, s) , and let $\phi: \mathcal{X} \rightarrow \mathbb{R}^d$ be a fixed feature map. Suppose we learn a linear quantile predictor $q_\alpha(x) = \langle \phi(x), w^* \rangle$ by minimizing the expected pinball loss under P :*

$$w^* \in \arg \min_{w \in \mathcal{W}} \mathbb{E}_{(x,s) \sim P}[\ell_\alpha(\langle \phi(x), w \rangle, s)].$$

Assume that the density ratio between Q and P satisfies:

$$\frac{dQ_\phi(\phi(x), s)}{dP_\phi(\phi(x), s)} = \langle \phi(x), v \rangle \quad \text{for some } v \in \mathcal{W}, \text{ and for all } (\phi(x), s) \in \text{supp}(Q_\phi).$$

Then the learned predictor q_α is calibrated under distribution Q at quantile level α :

$$\mathbb{E}_{(x,s) \sim Q}[\mathbf{1}\{s < q_\alpha(x)\} - \alpha] = 0.$$

This theorem implies that if the feature representation used in training expresses the density ratio between P and Q as a linear function, then the quantile predictor learned under P remains consistent under the shifted distribution Q . In the context of MIA, this ensures that the FPR remains at the target level α , even under distribution shift. The predictor $q_\alpha(x) = \langle \phi(x), w^* \rangle$ can be viewed as a neural network where $\phi(x)$ is the penultimate layer and w^* is the optimized final linear layer. This structure arises naturally from ERM, and the assumption of optimality in the last layer is mild, since the pinball loss is convex in w given fixed features.

Proof. As a first step, we prove by contradiction that the learned predictor q_α^* is $(\mathcal{W}, \phi, 0)$ -multi-accurate under P . Suppose not, then, by the definition of multi-accuracy, there exists some $w' \in \mathcal{W}$ such that

$$\mathbb{E}_{(x,s) \sim Q}[\langle w', \phi(x) \rangle \cdot (\mathbf{1}\{s < q_\alpha^*(x)\} - \alpha)] \neq 0.$$

Without loss of generality, suppose this expectation is strictly positive.

Since the pinball loss is convex and differentiable almost everywhere, its subgradient with respect to the weights at w^* is:

$$\nabla_w \mathbb{E}_{(x,s) \sim P}[\ell_\alpha(\langle w, \phi(x) \rangle, s)] \Big|_{w=w^*} = -\mathbb{E}_{(x,s) \sim P}[(\alpha - \mathbf{1}\{s < q_\alpha^*(x)\})\phi(x)].$$

Taking the inner product of this gradient with w' , we obtain:

$$\langle w', \nabla_w \mathbb{E}_P[\ell_\alpha(\langle w, \phi(x) \rangle, s)] \Big|_{w=w^*} \rangle = -\mathbb{E}_P[\langle w', \phi(x) \rangle \cdot (\alpha - \mathbf{1}\{s < q_\alpha^*(x)\})] < 0,$$

by assumption. Therefore, moving in the direction $-w'$ decreases the expected pinball loss objective, contradicting the optimality of w^* .

Thus, we must have:

$$|\mathbb{E}_{(x,s) \sim P}[\langle w, \phi(x) \rangle \cdot (\mathbf{1}\{s < q_\alpha^*(x)\} - \alpha)]| = 0 \quad \text{for all } w \in \mathcal{W},$$

i.e., q_α^* is $(\mathcal{W}, 0)$ -multi-accurate under P .

Finally, given that $\frac{dQ}{dP}(x)$ satisfies:

$$\frac{dQ_\phi}{dP_\phi}(\phi(x), s) = \langle \phi(x), v \rangle \quad \text{for some } v \in \mathcal{W}, \text{ with } \langle \phi(x), v \rangle > 0 \text{ for all } x \in \text{supp}(Q),$$

we can perform a change of measure from P to Q :

$$\begin{aligned} \mathbb{E}_{(x,s) \sim Q}[(\mathbf{1}\{s < q_\alpha^*(x)\} - \alpha)] &= \mathbb{E}_{(\phi(x), s) \sim Q_\phi}[(\mathbf{1}\{s < \langle \phi(x), w^* \rangle\} - \alpha)] \\ &= \mathbb{E}_{(\phi(x), s) \sim P_\phi} \left[\frac{dQ_\phi(\phi(x), s)}{dP_\phi(\phi(x), s)} (\mathbf{1}\{s < \langle \phi(x), w^* \rangle\} - \alpha) \right] \\ &= \mathbb{E}_{(\phi(x), s) \sim P_\phi} [\langle \phi(x), v \rangle (\mathbf{1}\{s < \langle \phi(x), w^* \rangle\} - \alpha)] \\ &= \mathbb{E}_{(x,s) \sim P} [\langle \phi(x), v \rangle (\mathbf{1}\{s < q_\alpha^*(x)\} - \alpha)] = 0 \end{aligned}$$

This completes the proof. \square

5.1 Empirical Estimates

To understand the implications of this theorem in our setting, we can treat the quantile regressor as a feature extractor using the final layer before the prediction step to generate embeddings $\phi(x)$ for each sample in the dataset. We compare the distribution over last-layer embeddings in the attack training set (the seen subset of classes) with the distribution over last-layer embeddings in the evaluation set. Intuitively, the transferability theorem states that when there exists a linear transformation between these two distributions, the false-positive-rate guarantee of the quantile regressor over the training distribution will also hold for the test (full) distribution.

Thus, in order to show that the theorem statement holds, we need to measure the density ratio between the attack training distribution and the test distribution. In practice, we approximate the density ratio using

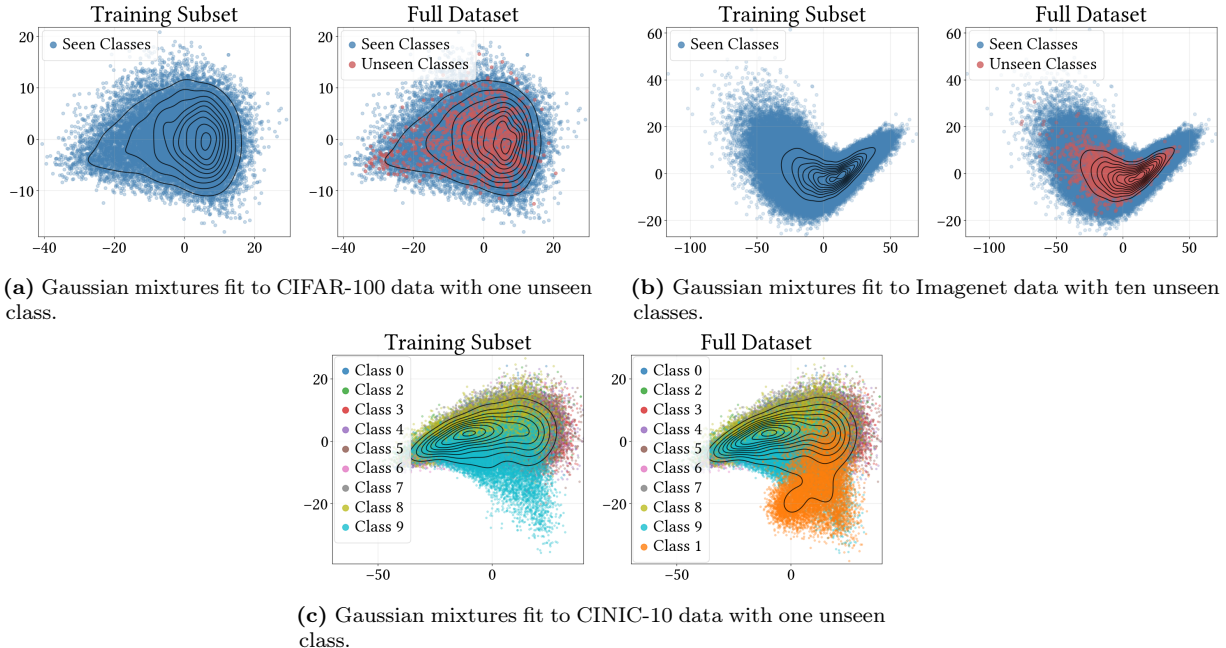


Figure 5: Visualization of Gaussian mixture models fit to the (dimension-reduced) embeddings learned by the quantile regression models trained on subsets of CINIC-10, CIFAR-100, and Imagenet. Dropping a class largely does not change the distribution over embeddings for CIFAR-100 and Imagenet, where we observe that quantile regression is the most effective.

Gaussian mixture models trained over a low-dimensional projection of the embeddings (the top two PCA components) rather than the original embeddings due to the relatively low sample size. These Gaussians are visualized in Figure 5.

Using these approximations, we explicitly measure the density ratio over the test set and fit a linear layer on top of the representation learned by the quantile regressor. We find that the linear fit improves as the dataset size and diversity increases: the MSE of the linear model on CINIC-10 is $8.11e-3$, on CIFAR-100 is $2.10e-3$, and on Imagenet $1.85e-3$. This experiment provides some validation of the empirical results we see in practice and may expect based on the visual representation of the image embeddings: the results of quantile regression are weakest on CINIC-10 (where the linear fit is comparatively worse) and best on ImageNet (where the linear fit is best).

6 Related Work

Membership inference attacks. Shadow models were proposed by Carlini et al. [2] to account for the inherent difficulty of memorizing some samples over others. Carlini et al. [3] study a number of membership inference attacks including shadow models in the context of diffusion models, showing that shadow models can achieve very high TPRs for diffusion models due to the amount of memorization.

Membership inference attacks based on quantile regression were introduced by Bertran et al. [1] for classification tasks. Follow-up work [13] extended this approach to the diffusion model setting using a score metric inspired by Duan et al. [4].

A number of earlier works propose using a single global score threshold across examples rather than fitting per-example thresholds [11, 18, 12, 4]. Later work [17, 2] has shown that these global score thresholds perform poorly compared to thresholds calibrated to example difficulty, particularly in the low-false positive rate regime.

MIA under distribution shift. A number of prior works have studied the effectiveness of membership inference attacks (in particular, shadow models) under varying distribution shift, although none of these study the unseen class setting that we study in our work. Yichuan et al. [19] study a setting in which the attacker has access to data encompassing a *superset* of the target labels, as well as attribute shift corresponding to

subpopulation reweighting. Liu et al. [9] augment shadow models with loss trajectories rather than scalar scores. They study distribution shift between CIFAR-10 and CINIC-10, which have the same label set. Galichin et al. [5] assume access to the same distribution as the target model and improve shadow models using knowledge distillation. Earlier works [2, 11] have empirically studied how shadow models perform when the target architecture or training procedure are not known exactly.

7 Discussion and Limitations

Our work makes significant progress toward membership inference attacks that can succeed in realistic settings where the attacker does not have access to significant subsets of the target model’s training distribution. We also systematically show limitations of shadow models in this setting.

Nevertheless, for such an attack to be useful in a real-world setting, particularly for black-box models, further work remains. We assume the attacker *does* have access to some samples to query at test time (albeit not enough to use in training the attack), which may or may not be a reasonable assumption. For instance, these queries may only be possible to make within the context of a law enforcement agency that has secure access to specific harmful content to query. In order for such an attack to be useful for non-specialist organizations such as model hosting services, significant challenges must be overcome in that they may not even have access to specific query examples.

We also note the limitations raised by [20] that membership inference attacks in real-world, black-box settings are limited because the model’s true training data is unknown. We view the practical utility of our attacks as being in the setting where an auditor may wish to flag a model for further manual scrutiny.

Acknowledgements

We are extremely grateful to Rebecca Portnoff for insightful discussions regarding realistic data access models for CSAM detection. Thanks also to Shuai Tang, Martin Bertran, and Matteo Boglioni for discussions on quantile regression attacks.

This work was supported in part by the National Science Foundation grants IIS2145670 and CCF2107024, and funding from Amazon, Apple, Google, Intel, Meta, and the CyLab Security and Privacy Institute. Any opinions, findings and conclusions or recommendations expressed in this material are those of the author(s) and do not necessarily reflect the views of any of these funding agencies. P.T. was supported by a Carnegie Bosch Institute fellowship. Z.S.W. was in part supported by NSF Awards #1763786 and #2339775.

References

- [1] Martin Bertran, Shuai Tang, Aaron Roth, Michael Kearns, Jamie H Morgenstern, and Steven Z Wu. Scalable membership inference attacks via quantile regression. *Advances in Neural Information Processing Systems*, 36:314–330, 2023.
- [2] Nicholas Carlini, Steve Chien, Milad Nasr, Shuang Song, Andreas Terzis, and Florian Tramèr. Membership inference attacks from first principles. In *2022 IEEE symposium on security and privacy (SP)*, pages 1897–1914. IEEE, 2022.
- [3] Nicholas Carlini, Jamie Hayes, Milad Nasr, Matthew Jagielski, Vikash Sehwal, Florian Tramèr, Borja Balle, Daphne Ippolito, and Eric Wallace. Extracting training data from diffusion models. In *32nd USENIX Security Symposium (USENIX Security 23)*, pages 5253–5270, 2023.
- [4] Jinhao Duan, Fei Kong, Shiqi Wang, Xiaoshuang Shi, and Kaidi Xu. Are diffusion models vulnerable to membership inference attacks? In *International Conference on Machine Learning*, pages 8717–8730. PMLR, 2023.

- [5] Andrey V Galichin, Mikhail Pautov, Alexey Zhavoronkin, Oleg Y Rogov, and Ivan Oseledets. Glira: Black-box membership inference attack via knowledge distillation. *IEEE Transactions on Information Forensics and Security*, 2025.
- [6] Ursula Hebert-Johnson, Michael P. Kim, Omer Reingold, and Guy N. Rothblum. Multicalibration: Calibration for the (computationally-identifiable) masses. In *Proceedings of the 35th International Conference on Machine Learning (ICML)*, volume 80, pages 1939–1948. PMLR, 2018.
- [7] Sayash Kapoor, Rishi Bommasani, Kevin Klyman, Shayne Longpre, Ashwin Ramaswami, Peter Cihon, Aspen Hopkins, Kevin Bankston, Stella Biderman, Miranda Bogen, et al. On the societal impact of open foundation models. In *International Conference on Machine Learning, Position Paper Track*, 2024.
- [8] Michael P. Kim, Christoph Kern, Shafi Goldwasser, Frauke Kreuter, and Omer Reingold. Universal adaptability: Target-independent inference that competes with propensity scoring. *Proceedings of the National Academy of Sciences*, 119(4):e2108097119, 2022. doi: 10.1073/pnas.2108097119. URL <https://www.pnas.org/doi/10.1073/pnas.2108097119>.
- [9] Yiyong Liu, Zhengyu Zhao, Michael Backes, and Yang Zhang. Membership inference attacks by exploiting loss trajectory. In *Proceedings of the 2022 ACM SIGSAC Conference on Computer and Communications Security*, pages 2085–2098, 2022.
- [10] Aaron Roth. Uncertain: Modern topics in uncertainty quantification. <https://www.cis.upenn.edu/~aaroht/uncertain.html>, 2022. Textbook, University of Pennsylvania.
- [11] Reza Shokri, Marco Stronati, Congzheng Song, and Vitaly Shmatikov. Membership inference attacks against machine learning models. In *2017 IEEE symposium on security and privacy (SP)*, pages 3–18. IEEE, 2017.
- [12] Liwei Song, Reza Shokri, and Prateek Mittal. Privacy risks of securing machine learning models against adversarial examples. In *Proceedings of the 2019 ACM SIGSAC conference on computer and communications security*, pages 241–257, 2019.
- [13] Shuai Tang, Zhiwei Steven Wu, Sergul Aydore, Michael Kearns, and Aaron Roth. Membership inference attacks on diffusion models via quantile regression. *arXiv preprint arXiv:2312.05140*, 2023.
- [14] David Thiel. Identifying and eliminating csam in generative ml training data and models. *Stanford Internet Observatory, Cyber Policy Center*, 23:3, 2023.
- [15] David Thiel, Melissa Stroebel, and Rebecca Portnoff. Generative ml and csam: Implications and mitigations. In *Stanford digital repository*. 2023.
- [16] Thorn and All Tech is Human. Safety by design for generative ai: Preventing child sexual abuse. <https://info.thorn.org/hubfs/thorn-safety-by-design-for-generative-AI.pdf>, 2024.
- [17] Lauren Watson, Chuan Guo, Graham Cormode, and Alex Sablayrolles. On the importance of difficulty calibration in membership inference attacks. *arXiv preprint arXiv:2111.08440*, 2021.
- [18] Samuel Yeom, Irene Giacomelli, Matt Fredrikson, and Somesh Jha. Privacy risk in machine learning: Analyzing the connection to overfitting. In *2018 IEEE 31st computer security foundations symposium (CSF)*, pages 268–282. IEEE, 2018.
- [19] Shi Yichuan, Olivera Kotevska, Viktor Reshniak, and Amir Sadovnik. Assessing membership inference attacks under distribution shifts. In *2024 IEEE International Conference on Big Data (BigData)*, pages 4127–4131. IEEE, 2024.
- [20] Jie Zhang, Debeshee Das, Gautam Kamath, and Florian Tramèr. Membership inference attacks cannot prove that a model was trained on your data. *arXiv preprint arXiv:2409.19798*, 2024.

A Experiments and Implementation Details

Shadow models were trained on 2 NVIDIA A100 GPUs using the code released by [2]. The code was used unmodified except to drop the relevant classes from the attack model training data.

The quantile regression models were trained on 4 A800 nodes, taking about 3000MB per node to train ConvNext-Tiny-224 models. Each model took as input a 224x224x3 image and returned 2 outputs, the predicted Gaussian mean and variance. Each model was trained for 30 epochs. For CINIC-10, training with no class dropout took approximately 40 minutes per model. For CIFAR-100, training took approximately 12 minutes per model. For ImageNet, training took approximately 5 hours per model. Under class dropout and sample dropout, the training dataset was smaller and training time reduced.

We also experimented with running ConvNext-Large-224, which took 11000MB per node to train, and significantly longer, i.e. 4 hours per model for CINIC-10.

B Additional Shadow Model Results

We provide additional results in the FPR 0.1% regime to supplement Figure 1.

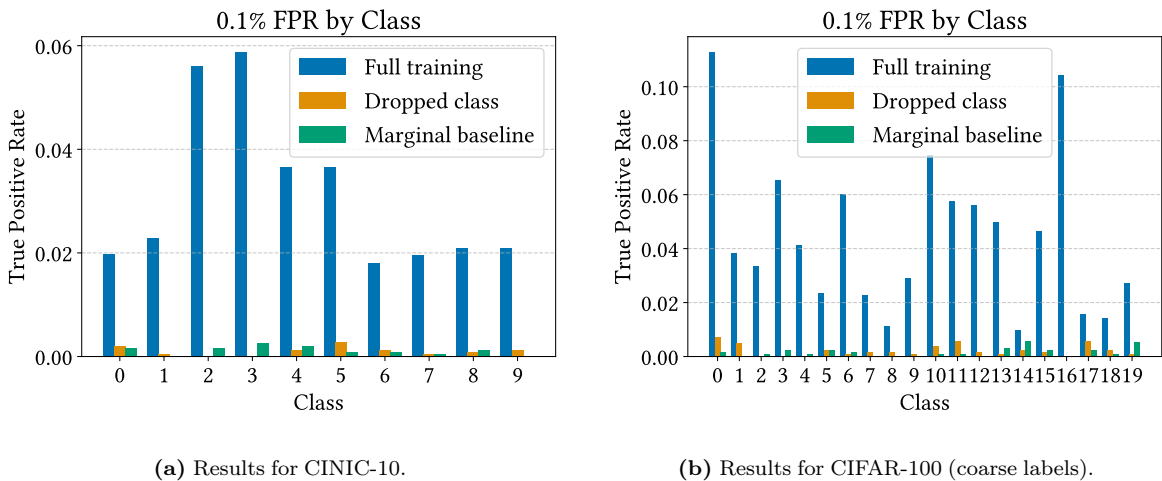


Figure 6: True positive rates for shadow model attacks in the 0.1% false positive rate regime for CINIC-10 and CIFAR-100. Each bar represents the TPR on the indicated class. In yellow, we plot the TPR when that class is excluded from shadow model training. The attack success degrades significantly under class exclusion, often performing worse than the marginal baseline (global threshold).